A cometary neutral gas simulator for gas dynamic sensor and mass spectrometer calibration

S. Graf, K. Altwegg, H. Balsiger, A. Jäckel, E. Kopp, U. Langer, W. Luithardt, C. Westermann, and P. Wurz

Physikalisches Institut, Universität Bern, Bern, Switzerland

Received 1 October 2003; revised 9 December 2003; accepted 19 December 2003; published 29 May 2004.

[1] The goal of the European Space Agency's Rosetta mission is a rendezvous with the Edgewood-Kuiper Belt comet 67P/Churyumov-Gerasimenko. After the initial encounter the spacecraft will accompany the comet for one to two years toward the Sun and throughout the perihelion passage. For the calibration of the onboard comet mass spectrometers a calibration system was built to simulate the neutral gas environment around a cometary nucleus. This facility consists of a fully automated three-chamber ultra-high vacuum system with a separate gas-mixing unit and a docking section with a five-axis table for instrument positioning and support. The gas-mixing unit produces mixtures of gases and also gas water vapor mixtures. The gas mixtures are fed into the vacuum system by a leak valve (static mode) or through a nozzle to form a molecular beam (dynamic mode). All flight and flight spare sensors of the Rosetta Orbiter Spectrometer for Ion and Neutral Analysis (ROSINA) have been calibrated in the static mode of the Calibration System for the Mass Spectrometer Instrument ROSINA (CASYMIR). Preliminary calibration measurements in a pressure range from 10^{-9} to 10^{-6} mbar for carbon dioxide and for noble gases from helium to xenon show very promising results. *INDEX TERMS:* 6005 Planetology: Comets and Small Bodies: Atmospheres—composition and chemistry; 6006 Planetology: Comets and Small Bodies: Atmospheres—evolution; 6062 Planetology: Comets and Small Bodies: Satellites; 6094 Planetology: Comets and Small Bodies: Instruments and techniques; *KEYWORDS:* comet, mass spectrometer, vacuum system

Citation: Graf, S., K. Altwegg, H. Balsiger, A. Jäckel, E. Kopp, U. Langer, W. Luithardt, C. Westermann, and P. Wurz (2004), A cometary neutral gas simulator for gas dynamic sensor and mass spectrometer calibration, *J. Geophys. Res.*, *109*, E07S08, doi:10.1029/2003JE002188.

1. Introduction

[2] The comprehensive calibration of space-probe instruments is both a very difficult and important task. Very often, the possibility to check the instrument sensitivities after its integration into the spacecraft is limited. The demands to the calibration of mass spectrometers in a comet mission are given by the volatile environment which is expected inside the coma around a cometary nucleus. In situ measurements at comet Halley [e.g., *Altwegg et al.*, 1999, and references therein] and several remote observations [e.g., *Crovisier and Bockelée-Morvan*, 1999, and references therein] have identified water as the main volatile component. Other minor constituents are, for example, CO, CO_2, and H_2CO. But species containing nitrogen and sulfur have also been found. The molecule density is expected to change over several orders of magnitude, depending on the spacecraft position and on the heliocentric distance of the comet. For comet Hale-Bopp water production rates between 10^{28} to 10^{31} s^{-1} have been published [e.g., *Colom et al.*, 1998; *Weaver et al.*, 1997, 1998; *Crovisier et al.*, 1997; *Crovisier*, 1998]. It is assumed that the expansion velocity for a water-dominated cometary coma is about 400 to 1000 m s^{-1} (see, for example, the work by *Lämmerzahl et al.* [1987] and *Combi et al.* [1999]). Such a velocity range yields densities between 10^{10} to 10^{16} m^{-3} around a distance of 1000 km from the nucleus. The coma composition will also depend strongly on the heliocentric distance of the comet as the activity of the nucleus decreases with increasing distance from the sun.

[3] For the calibration of mass spectrometers in a comet mission a system which can provide neutral beams of water vapor, both pure and with an admixture of minor gases is needed. It should also supply a wide range of pure gases and gas mixtures for calibration in dynamic and static atmospheres. In this paper we present the Calibration System for the Mass Spectrometer Instrument ROSINA (CASYMIR) which has been optimized with respect to the above mentioned problems and requirements. It can provide particle densities between 10^{13} to 10^{17} m^{-3} and molecular beam velocities of 300 to 3000 m s^{-1}.

[4] CASYMIR has been successfully used in the static mode calibration for a gas mass spectrometer instrument called the Rosetta Orbiter Sensor for Ions and Neutral

0148-0227/04/2003JE002188$09.00

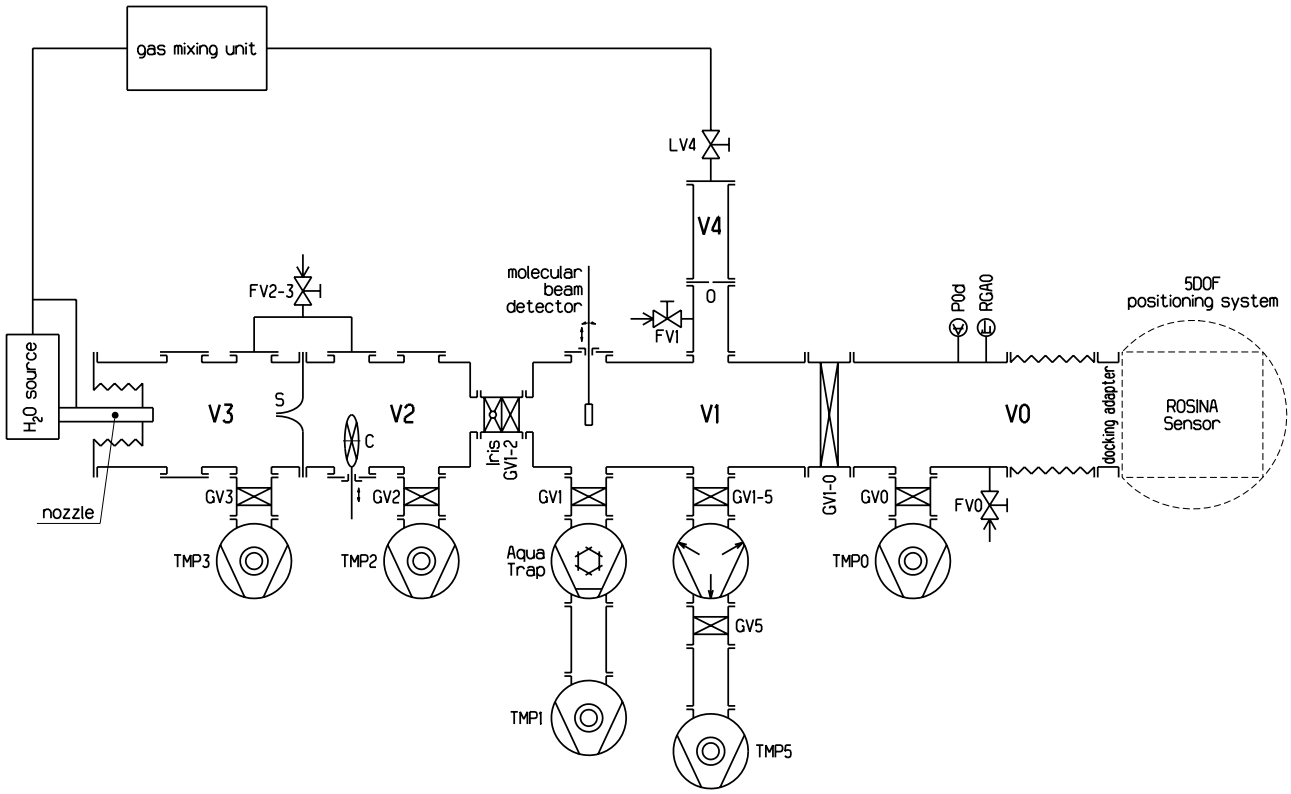

Figure 1. Schematic diagram of the ROSINA CASYMIR system. The main vacuum components are the bellows chamber with docking adapter V0, the main vacuum chamber V1, the collimator chamber V2, the expansion chamber V3, and the reference chamber V4. Gate valves are labeled with GV and the chamber number. The Stabil-Ion reference gauge P0d and the residual gas analyzer RGA0 are mounted inside V0. Chambers V0 to V3 are pumped by individual turbomolecular pumps, TMP0 to TMP5. Additional components are the skimmer S, the chopper disk C, and the orifice O between V4 and V1. The venting valves FV0 to FV2-3 are connected to a nitrogen supply line.

Analysis (ROSINA) [cf. *Balsiger et al.*, 1997, 2004] on the European Space Agency's Rosetta mission to comet 67P/Churyumov-Gerasimenko [*Berner et al.*, 2002]. The ROSINA instrument package consist of three sensors, two mass spectrometers to measure cometary ions and neutrals and a pressure gauge assembly:

[5] 1. The Double Focusing Mass Spectrometer (DFMS) is a high-resolution mass spectrometer in Nier-Johnson configuration [*Johnson and Nier*, 1953] with a wide dynamic range and a good sensitivity. It has a mass range of 12–140 amu/e and a mass resolution of $m/\Delta m > 3000$ at the 1% peak height (m/q = 28), which corresponds to a resolution of $m/\Delta m \sim 7000$ at the 50% level.

[6] 2. The Reflectron Time-Of-Flight mass spectrometer (RTOF) complements DFMS with an extended mass range from 1 to >300 amu/e and with a higher sensitivity. The unique advantage of time of flight instruments is that they have no limits in the mass range. A spectrum of the entire mass range is recorded at once and is only limited by the signal accumulation memory. The long ion drift path of 3.6 m in the triple reflection mode yields a mass resolution (full width at half maximum) of $m/\Delta m > 4000$ at the 50% peak height level.

[7] 3. The COmetary Pressure Sensor (COPS) consists of two gauges based on the extractor-type ionization gauge principle. One gauge measures the total number density and the other one the ram pressure, which is equivalent to the cometary gas flux. Combining the results from both gauges and the known spacecraft orientation relative to the comet nucleus the gas velocity can be calculated.

[8] Section 2 presents an overview of the CASYMIR system and its performance followed by some critical measurements in section 3. Applications of CASYMIR to the first ROSINA neutral gas calibration campaign are reported in section 4. Therein selected static mode measurements of the three ROSINA instruments with CO_2 and various noble gases (He, Ne, Ar, Kr, and Xe) within a pressure range from about 10^{-9} mbar to 10^{-6} mbar are presented. Mainly results from the Flight Spare models (FS) will be given, as these are the instrument models which are integrated in the Rosetta spacecraft. The Flight Models (FM) will be used in the laboratory for reference, software tests, and further calibration.

2. Overview of the System

[9] A detailed description of most parts of the CASYMIR system is given in the work of *Westermann* [2000] and *Westermann et al.* [2001]. Figures 1 and 2 show a schematic drawing and a picture with the main components, the Gas Mixing Unit (GMU), the vacuum system and the docking interface with the 5-axis table (5DOF

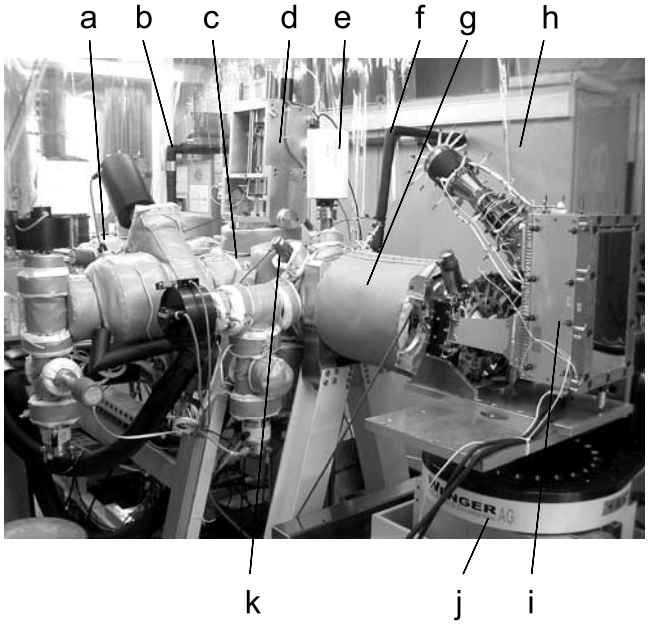

Figure 2. Picture of the CASYMIR calibration facility showing the following components: (a) vacuum chambers V3 and V2, (b) gas supply tube from the GMU toward the nozzle, (c) main chamber V1, (d) movable support for the beam detector system, (e) residual gas analyzer RGA0, (f) gas supply tube toward the leak valve, (g) docking section with bellow chamber, (h) back side of the GMU, (i) DFMS, (j) 5-axis table with instrument support, and (k) Stabil-Ion reference gauge.

positioning system). The GMU provides a wide variety of gases and mixtures thereof to the vacuum system either through the beam nozzle or through the leak valve LV4. Inside the GMU four gas inlet tubes and two liquid vaporizers are simultaneously connected to a gas-mixing volume. Each flow can be varied by a mass flow controller with a maximum flow rate between 10 to 100 sccm (standard cubic centimeters per minute). The liquid reservoirs are filled with water and methanol whereas the gas inlet tubes are connected to CO_2 and various noble gases.

[10] After passing through the mixing volume the neutral gas enters the vacuum system through the leak valve LV4 into the reference chamber V4 for static mode calibration. For the dynamic mode calibration there is an additional gas supply tube from the mixing volume toward the nozzle, which is mounted into the expansion chamber V3. The nozzle is movable in both dimensions perpendicular to the beam axis as well as along the beam axis.

[11] During static mode measurements only the main chamber V1 and the bellows chamber V0 are used. In order to calibrate the ROSINA instruments they are mounted on the positioning system. This is a movable table with five degrees of freedom, three translations and two rotations. Then they are connected to CASYMIR via the docking adapter which is located on the right end of the bellows chamber V0, see also Figures 1 and 2. To facilitate the instrument exchange, V0 can be sealed off from the main chamber V1 and the whole vacuum system by the gate valve GV0-1. A separate flush valve FV0 and pump system TMP0 allow to flush only the bellows chamber and to pump it again. Because the molecular beam is not used in the static mode experiments gate valve GV1-2 is also closed to reach the lowest possible residual gas level. Depending on the instrument at the docking interface residual gas pressures down to 3×10^{-10} mbar are possible, measured with the Granville-Phillips Stabil-Ion (Helix Technology Corporation: Series 370) reference ionization gauge, labeled with P0d in Figure 1. The Residual Gas Analyser RGA0 is a Balzers QMS 200 mass spectrometer.

[12] The second experiment setup uses a molecular beam to simulate a dynamic environment, e.g., the expansion of a cometary coma. The switch-over between static and dynamic setup can be performed without any changes at the docking interface. Only a small repositioning of the sensor, done with the movable table, could be necessary to bring the sensor entrance system into the center of the molecular beam. The construction of the bellows chamber and the table allows also for different orientation of the sensor source system with respect to the molecular beam axis or scanning through the molecular beam. The instrument source system can be rotated about 12° to 15° out of the molecular beam axis.

[13] To achieve a well defined beam profile a two chamber setup (collimator chamber V2 and expansion chamber V3) with skimmer, which is used to extract the central part of the beam, and an iris diaphragm is implemented along the molecular beam axis. The skimmer is integrated between chamber V2 and V3, whereas the iris diaphragm is located in front of gate valve GV1-2. The beam profile can be scanned with the molecular beam detector system, located in the main chamber, in one or two dimensions. The molecular beam detector system consists of a fast ion gauge (R.M. Jordan Co.) and a cross beam deflector ionizer (ABB Extrel). In combination with the chopper disc, integrated in the collimator chamber V2, measurement of the beam velocity is possible.

[14] The vacuum system can be controlled by a control and data acquisition system consisting of two PC/Linux systems. The software is divided into two major parts: (1) The task of the first part is to control all the hardware devices of the CASYMIR system and to acquire the data generated. The communication between the computer system and the CASYMIR devices is done over serial interfaces and each device is controlled by its own job running on the Linux system. The collected data from all these jobs are written in a shared memory area. (2) The second part is a Java based Graphical User Interface (GUI). The implementation in this programming language allows the GUI to run on any computer system that provides a Java virtual machine and is connected to the internet. The communication between both systems runs through the TCP/IP protocol. An additional job exchanges information between the shared memory area and the GUI.

3. Performance of the System in the Dynamic Mode

[15] The $AlCuMg_2$ alloy chopper disc integrated into the collimator chamber V2 allows, together with the fast ion gauge from the beam diagnostic system, the measure-

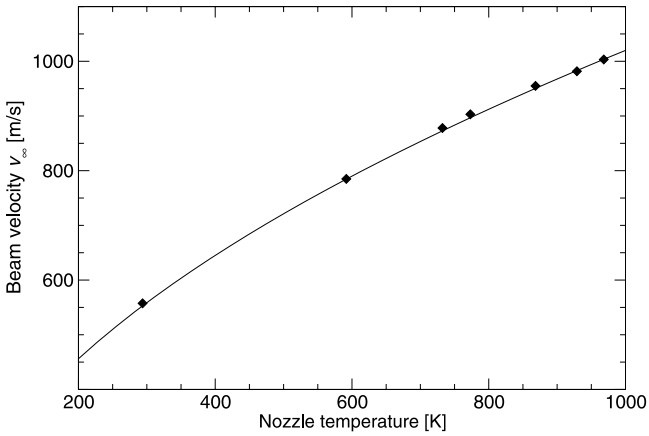

Figure 3. Argon beam velocity as a function of the nozzle temperature. The black diamonds represent the measured beam velocities. The solid line shows the expected theoretical curve.

ment of the beam velocity. The terminal beam velocity v_∞ depends on the species in the beam (with mass m and $\gamma = C_p/C_v$) and the nozzle temperature T_0 [*Ashkenas and Sherman*, 1966; *Scoles*, 1988]:

$$v_\infty = \sqrt{2\frac{\gamma}{\gamma - 1}\frac{kT_0}{m}}. \quad (1)$$

The temperature of the CASYMIR nozzle can be set between 300 and 900 K. Figure 3 shows the excellent agreement over the whole temperature range between equation (1) and the experimentally determined terminal velocities for an argon molecular beam.

[16] As the beam detector system is mounted on a movable mechanical arm perpendicular to the molecular beam axis, beam profiles in two dimensions can be measured. Figure 4 shows a set of beam profiles for two different nozzle pressures (58 and 105 mbar) and two iris diaphragm diameters (2.4 and 3.7 mm). The profiles are not

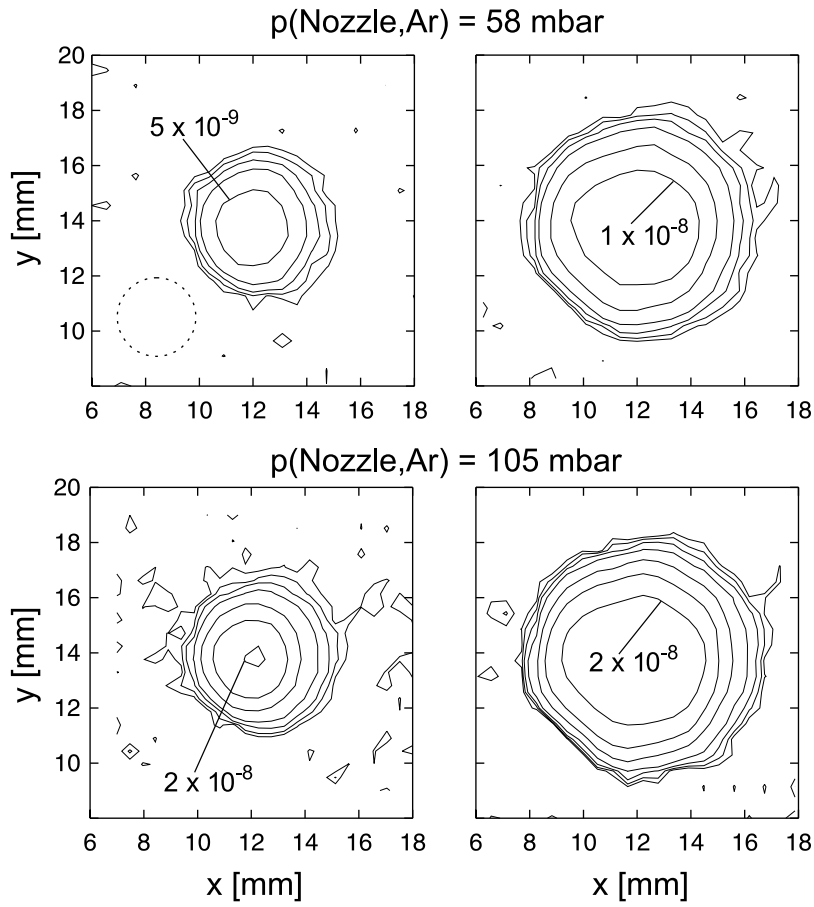

Figure 4. Pressure contour plots for argon molecular beams with different nozzle pressure and iris diameter. Contour lines are drawn at the following pressure levels: 2×10^{-10}, 5×10^{-10}, 10^{-9}, 2×10^{-9}, 5×10^{-9}, 10^{-8}, and 2×10^{-8} mbar. The highest pressure level is labeled in each plot. The two plots on the left-hand side were measured with an iris opening of 2.4 mm, whereas the plots on the right-hand side are the results with an iris diameter of 3.7 mm. The dashed circle in the top left panel shows the source opening of the beam diagnostic system.

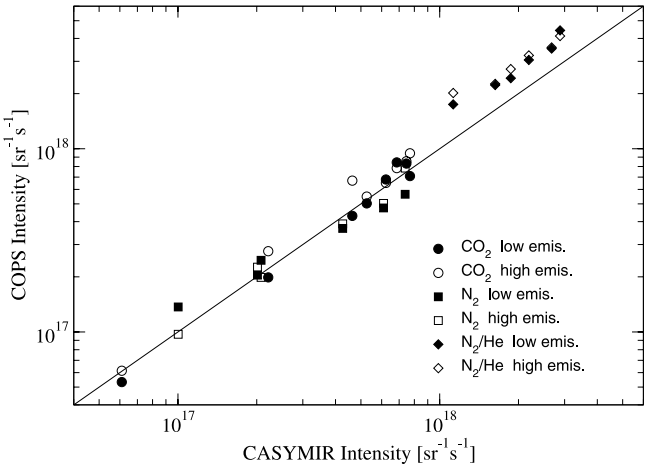

Figure 5. Molecular beam intensities measured with the CASYMIR beam diagnostic system and the COPS Engineering Qualified Model (COPS-EQM). Open symbols denote results from COPS-EQM in the high-emission mode; full symbols are from the low-emission mode.

corrected for the source opening of the ionizer. One-dimensional measurements including deconvolution have shown a correction for the beam diameter of around 3 mm [see also *Westermann*, 2000]. As the beam diameter is larger than the ionizer source opening, no correction for the maximum beam intensity is necessary.

[17] Beam profiles can also be used to calculate beam intensities. Figure 5 shows the comparison between intensities measured with the ionizer of the beam diagnostic system and the COPS engineering qualification model sensor, COPS-EQM. Note, that the distance from the nozzle to the COPS-EQM is not the same as from the nozzle to the beam diagnostic system. In order to compare both sets of results the intensities have been given in particles per second and steradian. A good agreement was found for N_2 and CO_2, squares and circles in Figure 5. Results from both COPS emission modes are plotted. In the high-emission mode an electron emission current of 100 μA is used for the measurements, whereas in the low-emission mode only 15 μA are generated. A systematic offset of about 35% is shown when a 1:1 mixture between N_2 and He was used. This can be explained as a characteristic of gas mixtures in free jet expansion which pushes away the lighter gas component from the central beam axis [*Scoles*, 1988]. As the COPS-EQM sensor measures the beam intensity further downstream of the molecular beam, the composition is no longer identical compared to the one at the beam diagnostic system. Moreover, most probably there is an enrichment in the heavier gas component, nitrogen, which has a higher ionization cross section than helium. Therefore the uncorrected measured beam intensities at the position of the instrument docking plate should be higher compared to the CASYMIR cross beam deflector results.

4. Calibration Measurements

4.1. Introductory Remarks

[18] In the following subsections we present some preliminary calibration results for the three ROSINA sensors. These results derive from neutral gas experiments in a static environment. For ion measurements a low-energy source is presently designed and built. But this source will be integrated into another calibration facility [*Ghielmetti et al.*, 1983], and the results will be presented later. Although static measurements do not correspond directly to the results from an expanding cometary coma they are needed to fully understand the sensor performance. Furthermore they are also a necessity to do the dynamic calibration as there will be always a static background during a molecular beam setup. Such dynamic measurements with a gas beam are presently performed with the DFMS-FS sensor. Another important point will be the comparison between FM and FS calibration. New calibration results, which are obtained in the laboratory with the FM model sensor have to be translated to calibration factors for the FS models on the spacecraft in order to evaluate the in-situ measurements from the target comet.

[19] The chosen calibration gases had to fulfill important criteria, in particular to avoid any possible contamination and memory effects in the sensor and detector systems by using low abundant cometary gas constituents for the calibration. If possible the used calibration gases should represent the mass range of the sensor. Therefore the following species were selected: He, CO_2, and Kr for RTOF; Ne, CO_2, and Xe for DFMS and argon for COPS. The noble gases have been chosen due to their inert properties, different atomic masses and isotopic patterns. Carbon dioxide represents a medium mass and allows the investigation of fragmentation in the ion source. The above gas selection covers the full mass range of the DFMS, but with the given constraints it is not possible to cover the full mass range of the RTOF sensor.

[20] For in-flight optimization and mass calibration both mass spectrometers are equipped with an onboard Gas Calibration Unit (GCU). This unit consist of two small tanks filled with a gas mixture of the above mentioned calibration gases. The mixture for RTOF contains He:CO_2:Kr (1:1:1). For DFMS the mixture is CO_2:Ne:Xe (92.8:4.5:2.6 Mol%) and additional 0.1 Mol% He for leak testing purposes. With the use of the integrated mini Pirani pressure sensor of the GCU, sensitivity calibration measurements should also be possible. Further details about the GCU design and its operation are given in the work of *Matuschek et al.* [2001a, 2001b].

4.2. RTOF

4.2.1. Instrument Characteristics

[21] The ROSINA reflectron time of flight mass spectrometer has been especially designed for the Rosetta mission. This instrument operates by simultaneous extraction of ions from the ionization region into a drift tube. The mass resolution is a function of the total drift time and the temporal spread of the ion packets at the location of the detector.

[22] The RTOF sensor (Figure 6) can be divided into four different parts. The first part is the source region with two independent ion sources. The first source, the electron impact ion Storage Source (SS), ionizes neutral particles, stores these ions for 100–500 μs, and extracts them by a short high-voltage pulse into the time of flight system. The

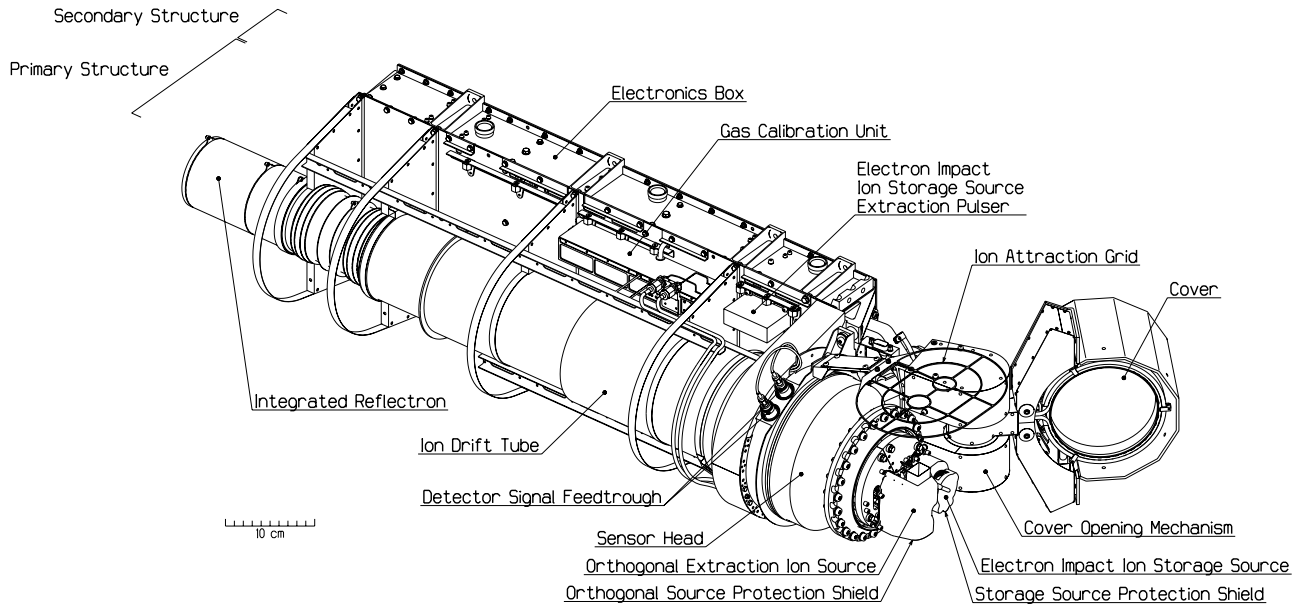

Figure 6. Three-dimensional drawing of the RTOF flight sensor (without high voltage protection foil) showing the primary structure with the ion optics and the secondary structure representing the electronics box.

second source, the Orthogonal extraction ion Source (OS), directs incoming ions (ionized externally of the RTOF sensor) into the acceleration field perpendicular to their incoming velocity vectors, again by means of a high-voltage pulse. Both sources contain a double filament assembly for redundancy reasons. The SS is optimized for the neutral part of the cometary coma, whereas the OS is optimized for ions, but can also be used in the other mode [*Balsiger et al.*, 2004].

[23] The second part of the sensor is the time of flight section, which consists of the field-free drift path (approximately 1 m long) and two ion mirrors, the integrated reflectron [*Scherer*, 1999] and the hard mirror [*Hohl et al.*, 1999], located on a common axis and facing each other for multiple reflections of the ion trajectories.

[24] Thirdly, the RTOF sensor includes two separate MCP (Multi Channel Plate) detectors, one for the SS detector and one for the OS detector [*Schletti et al.*, 2001].

[25] The fourth part of RTOF is the electronic box that houses eight electronics boards. Two data acquisition systems, i.e., Equivalent Time Sampling (ETS) and Equivalent Time Sampling Light (ETSL) are responsible for the data recording and the data readout from the two sources. Both are based on time to digital signal processing technique. The main difference between these two boards, which are both designed for fast and non-repetitive signal pulses, is the existence of analog to digital converters on the ETS board in contrast to the ETSL. Therefore the ETS detector can be run in an analog mode to handle high ion fluxes. More information about the data acquisition systems is provided in the technical report of *Loose* [2002].

[26] Depending on various mission conditions several operation modes had been designed to assure optimized scientific data acquisition. RTOF will perform measurements in the following operational modes: shutter mode, optimization mode, calibration mode (self calibration of the instrument), blank mode, and the two cometary modes (gas and ion). Subsequently, only the cometary modes will be described in more detail, since the other measurement modes are irrelevant for the instrument calibration in the laboratory. The gas mode refers to neutral particles of the coma, the ion mode refers to ionized particles. The SS will normally be run in the gas mode, the OS in the ion mode, but in order to use the calibration facility both channels are run in the gas mode.

[27] As described above, the sensor can measure in single or in triple reflection mode. The single reflection mode refers to ion trajectories starting at the ion source, being one time reflected in the reflectron and ending at the detector. The spectra achieved with the single reflection mode will have a lower resolution but higher sensitivity. In the triple reflection mode, the ions leave the ion source, reverse their direction of motion for the first time in the reflectron, and experience a second reflection in the hard mirror. After a further reflection in the reflectron, they will finally hit the detector. By enhancing the time of flight path the mass resolution in the spectra will also be increased. Switching between single and triple reflection mode can easily be achieved by changing the voltage settings at the reflectron lens. Both, gas and ion mode, can operate simultaneously but only in the same reflection mode because of the commonly used reflectron structure and the differing voltage settings for the single and triple reflection.

[28] In conclusion, the RTOF sensor contains two similar but independent source-detector subsystems in one common structure. These subsystems share the principal ion-optical components, the integrated reflectron and the hard mirror. The ion sources, the detectors and the data acquisition systems are separate. This configuration guarantees high reliability by almost complete redundancy. For more ex-

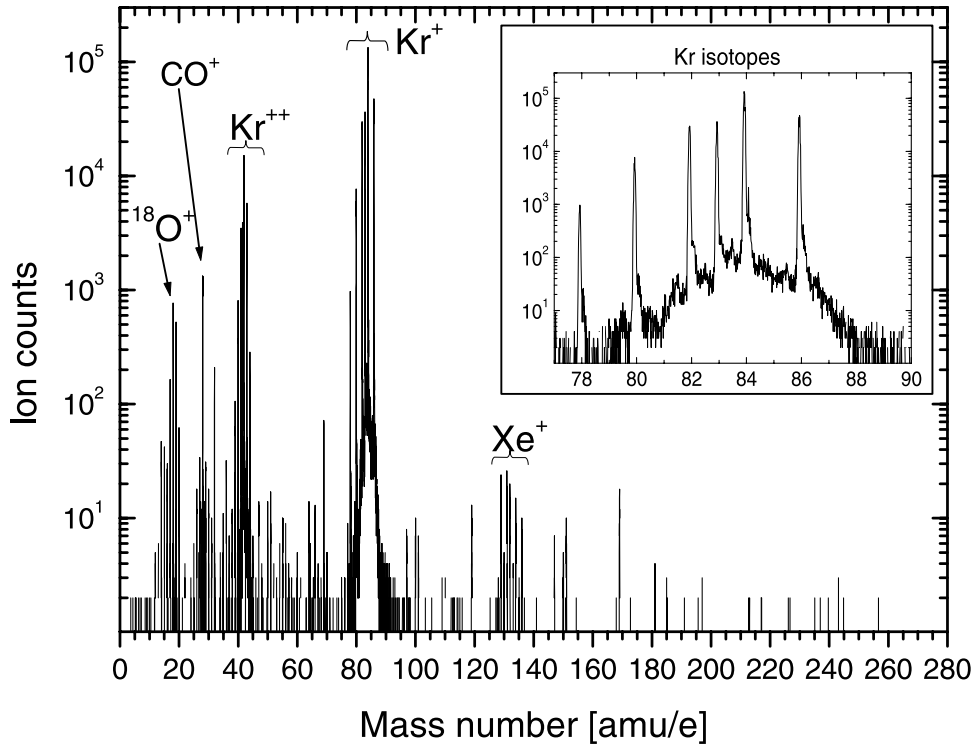

Figure 7. Typical RTOF mass spectrum in the mass range from 1 to 280 amu/e. The data are taken over a period of 200 s and cover a dynamic range of 5 orders of magnitude. The detailed view shows the Kr isotopes mass spectrum.

plicit information about the RTOF sensor characteristics see also A. Jäckel et al. (manuscript in preparation, 2003).

4.2.2. Preliminary Calibration Results

[29] Until now, two static mode calibration periods had been performed with the RTOF instrument. The first period took place in April 2002 with the RTOF-FS model and the second calibration session was performed with the RTOF-FM instrument during January 2003. With a special adapter the RTOF sensor is flanged to the docking interface of the CASYMIR chamber V0. The RTOF sensor is pumped by CASYMIR via the instrument sensor head. The typical residual gas pressure that is reached at CASYMIR is less than 5×10^{-9} mbar. In order to determine key parameters (e.g., sensitivity, dynamic range, and reproducibility) for the sensor, measurements at the following pressure values were performed: 5×10^{-9}, 10^{-8}, 10^{-7}, and 10^{-6} mbar. Two identical instruments, the flight sensor and the reference model, provide the opportunity to compare measurements of both sensors, as well as to predict measurements that will be performed in the comets environment.

[30] Figure 7 represents a typical RTOF-FM mass spectrum of krypton sample gas taken at a pressure of 10^{-7} mbar. Additionally to the Kr isotopes it is possible to identify various other mass lines, e.g., $^{18}O^+$, the mass line 28, that corresponds to CO^+, $^{14}N_2^+$ and $C_2H_4^+$, and the xenon isotope group. The source of the Xe peaks is a marginal contamination of the Kr gas. The measurement was performed using the OS and the single reflection mode, i.e., mode 513, with an acquisition time of 200 s. The spectrum was recorded with a repetition rate of 10 kHz. In this spectrum, the dynamic range that depends mainly on the accumulation time and the signal-to-noise ratio covers 5 orders of magnitude. The integrated counts over the main krypton mass peak result in a ^{84}Kr sensitivity of 1.4×10^{-4} mbar^{-1}.

[31] Figure 8 shows krypton isotopic ratios measured with the RTOF-FM instrument using three modes (mode 503, 513, and 523). The only difference between these three modes is the variation of the filament emission current from 20 μA in mode 503, to 100 μA (mode 513) and to 200 μA in mode 523. They are all single reflection spectra taken with ETSL and ionized and accelerated with the OS respectively. The isotopic ratios, especially for the ratios $^{78}Kr/^{86}Kr$, $^{80}Kr/^{86}Kr$,

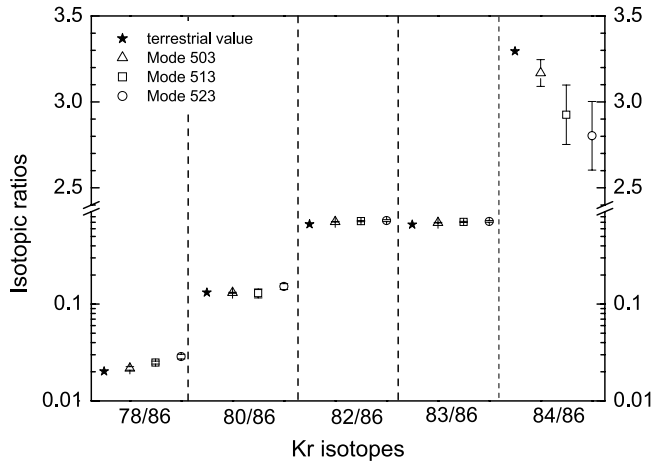

Figure 8. RTOF krypton isotopic ratios normalized to ^{86}Kr compared to the theoretical terrestrial values. Each data point represents 15 measurements taken at various pressure values: 5×10^{-9}, 10^{-8}, 10^{-7}, and 10^{-6} mbar.

$^{82}Kr/^{86}Kr$, and $^{83}Kr/^{86}Kr$ reflect very well the expected terrestrial isotopic ratios. The increasing error bars for the $^{84}Kr/^{86}Kr$ results at higher emission values are explainable because of a saturation effect within the ETSL. Due to the ETSL effective dead time of 133 ns some counts of very high intensity measurements are lost. Therefore the ^{84}Kr peak is underestimated compared to the other Kr isotopes.

4.3. DFMS

4.3.1. Instrument Overview

[32] The second ROSINA sensor is a compact state of the art high-resolution mass spectrometer. It is a classical double-focusing mass-spectrometer [*Mattauch and Herzog*, 1934] designed in Nier-Johnson configuration [*Johnson and Nier*, 1953, and references therein]. A full description is presented in the work of U. Langer et al. (manuscript in preparation, 2003) and by *Balsiger et al.* [2004].

[33] The principal separation of ions is achieved by a deflection of 90° in an electrostatic analyzer, which is followed by a magnetic deflection of 60°. The electrostatic analyzer is made up of a pair of deflection plates with a toroidal shape. The subsequent magnetic analyzer consists of a sector magnet (0.35 T). The DFMS covers a mass range from 12 amu/e (C^+ ions) to about 140 amu/e (xenon isotopes). It exhibits a mass resolution at 1% peak height of up to 3000, which allows the spectrometric separation of, e.g., ^{13}C and ^{12}CH or CO and N_2. Figure 9 shows an image of the fully assembled DFMS-FS without the surrounding Multi Layer Insulation (MLI). The FS model is the one, which has been integrated onto the Rosetta spacecraft in July 2002.

[34] The DFMS can be run in two different modes. On the one hand it will investigate the already ionized gas components of the comet and on the other hand it will analyze the cometary neutral gases with the aid of a classical electron impact ion source. This ion source is equipped with two independent filaments, which provide redundancy and should guarantee its functionality for the whole mission period. The electron energy for ionization can be varied between about 17 eV and 90 eV.

[35] By means of an electrostatic switch the ion beam can be guided through two different slits previous to the electrostatic analyzer: a 14 μm-wide slit for high-mass resolution and a 200 μm-wide slit for low-mass resolution (and thus more sensitive) measurements.

[36] For varying purposes three different detectors are available: a MCP, a Channel Electron Multiplier (CEM) and a Faraday cup (FAR). The main imaging detector is the one-dimensional position sensitive MCP detector. This position sensitive detector consists of two MCPs placed in chevron configuration, together forming a rectangular array of amplifying channels. Detector readout will be accomplished by two independent Linear Electron Detection Arrays (LEDA). When using the MCP detector a zoom optic allows to enlarge the ion beam in front of the detector and thus maintain the sensor's mass resolution. The channeltron detector acts mainly as a redundant detector and is particularly used for high-resolution spectra. The Faraday cup provides the needed long-term stability to cross-calibrate the other detectors with the help of the calibration gas from the GCU. The one-dimensional MCP detector allows to detect a certain part of the whole mass spectrum at once. When using the two other detectors the ion beam has to be scanned over the corresponding detector slits in order to obtain a single mass peak. A complete standard spectrum over the whole mass range taken with the MCP or the CEM detector needs about 10 min or three hours, respectively. Individual mass peaks (e.g., high-resolution cutouts) can be measured in time intervals of approximately one minute.

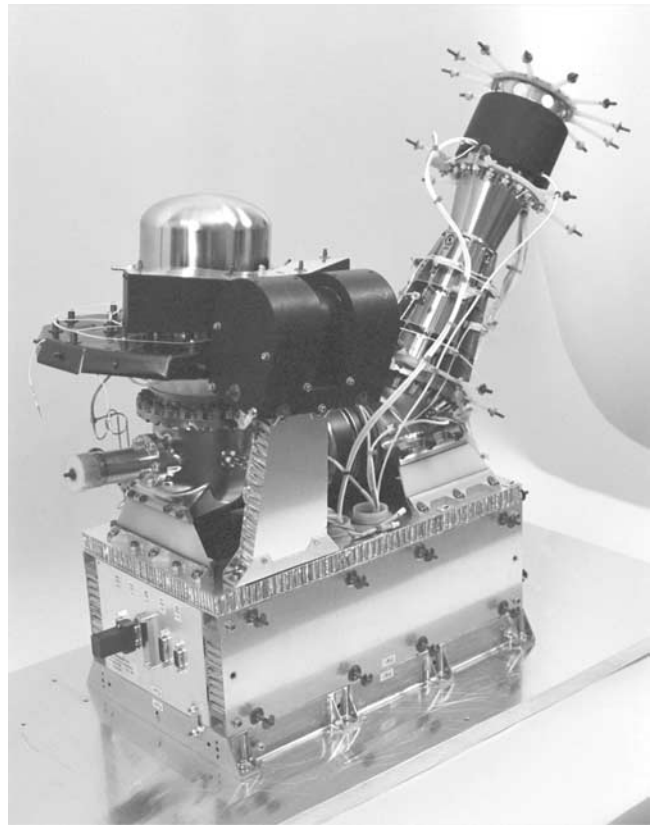

Figure 9. Picture of the ROSINA DFMS-FS model without the surrounding multilayer insulation. The electronics are integrated in the lower box, which has a length of 40 cm. The upper part shows the actual sensor system with the ion optics: the upper left part consists of the ion source with its protection cover, the middle part houses the electrostatic analyzer and the sector magnet, and in the upper right part the detector housing and its electronics are identifiable.

4.3.2. Preliminary Calibration Results

[37] The main pre-flight calibration campaign of the double-focusing mass spectrometer has been performed in June 2002. During this campaign the DFMS-FS sensor has been mounted with a special adapter onto the CASYMIR facility and was pumped through its ion source by the 1000 l s^{-1} pump TMP1 of the V1 chamber. In this configuration residual gas pressures in V1 were approximately 5×10^{-9} mbar. The DFMS calibration has been accomplished in a quasi-static mode, where the sensor is immersed in a neutral gas of known pressure. The used gases were on one side the calibration gas mixture and on the other side its specific components: CO_2, Ne and Xe. During this calibration the sensitivities for the main mass/charge peak in different modes for each detector and for

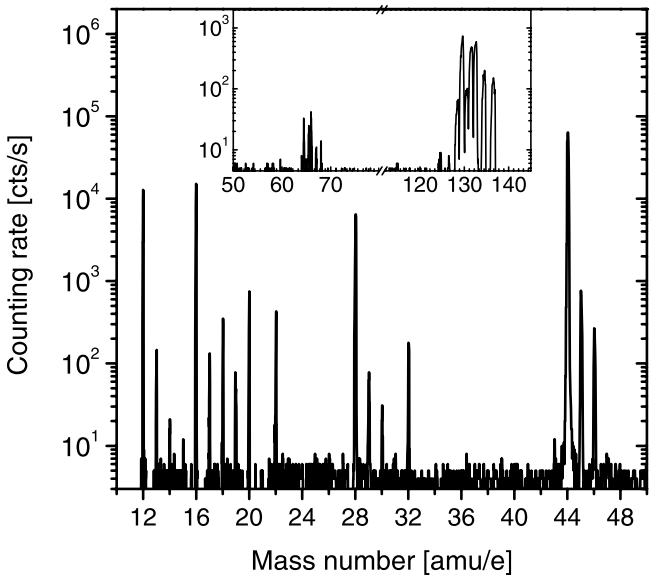

Figure 10. DFMS mass spectrum of the calibration gas (CO_2, Ne, and Xe) at 5×10^{-7} mbar, taken in low resolution with filament 1 (emission current = 20 μA) and the CEM detector. Whereas the larger panel displays mainly the mass peaks of CO_2, Ne, and the residual gas, the inner panel shows the higher mass peaks of Xe.

the given gases were derived. This main peak sensitivities S_{main} depend on the selected gas (e.g., due to different ionization cross sections), the used detector (e.g., due to different detector gains), the ion transmission probability, and the electron current in the ion source. Additionally, selected isotopic ratios and fragmentation patterns were determined. The performance of the gas calibration unit was also investigated.

[38] Figure 10 shows a typical mass spectrum of the used gas mixture at 5×10^{-7} mbar. The spectrum has been taken in the low-mass-resolution mode with the CEM detector and filament 1 at 20 μA. Figure 10 clearly demonstrates the ability of the DFMS to measure the specified mass range from 12–140 amu/e. The larger panel displays mainly the mass peaks of CO_2 (m/q = 12, 16, 22, 28, and 44), Ne (m/q = 20 and 22) and the residual gas. The inner panel shows the higher mass peaks of the single and double charged Xe ions. The presented spectrum covers a dynamic range of four magnitudes. As a matter of fact the DFMS sensor features an effective dynamic range of up to eight magnitudes.

[39] In order to determine the sensor sensitivities three main quantities are needed. The first quantity is the ion current I_{main} determined from the main mass/charge peak of the selected gas. The second parameter is the electron emission current I_e from the ion source. The third quantity needed is the gas pressure p which is computed from the quasi-static pressure measured during the calibration. This pressure is obtained from a Granville-Phillips Stabil-Ion gauge at the input to the mass spectrometer. Accordingly, the DFMS sensitivity values S_{main} have been determined for the main mass/charge peak of each gas from the following equation:

$$S_{main} = \frac{I_{main}}{I_e \cdot p}. \quad (2)$$

Table 1 shows measured main peak sensitivity values for three different calibration gases, the two filaments, and for all three detectors in high- and low-resolution modes. Generally, it could be proved that the DFMS sensitivity is independent of the ion source pressure in the investigated range of 10^{-8}–10^{-6} mbar. The presented results are therefore mean values from multiple measurements at different pressure settings. Except for xenon the results for filament 2 are typically three times higher than for filament 1. This fact seems to be caused by asymmetries in the ion source and imperfect optimization of the ion source settings for filament 1, which is still under close investigation. Figure 11 displays the sensitivity values for CO_2 (m/q = 44) as a function of the three possible electron emission currents (2, 20, and 200 μA). It is visible that an increase of the emission current causes generally a decrease of the sensor sensitivity compared to the theoretically expected rise (dotted lines). As the chosen calibration pressures and DFMS settings could not lead to saturation effects a possible explanation is a change in the field configuration of the ion source at higher emissions. This may cause a worse extraction of the produced ions.

4.4. COPS

4.4.1. Instrument Overview

[40] COPS is the third sensor of the ROSINA instrument package. Figure 12 shows the FS model with the two

Table 1. DFMS-FS Main Mass Peak Sensitivity Values for Three Different Calibration Gases, for the Two Filaments, and for All Three Detectors in High- and Low-Mass Resolution[a]

Gas	CEM Low Resolution MCP	CEM Low Resolution	CEM Low Resolution FAR	CEM High Resolution MCP	CEM High Resolution	CEM High Resolution FAR
			Filament 1			
CO_2	1.3×10^{-2}	1.1×10^{-2}	1.5×10^{-2}	1.2×10^{-3}	1.1×10^{-3}	1.6×10^{-3}
Ne	4.2×10^{-3}	4.1×10^{-3}	5.6×10^{-3}	2.9×10^{-4}	2.7×10^{-4}	5.6×10^{-4}
Xe	2.8×10^{-2}	1.5×10^{-2}	2.0×10^{-2}	4.8×10^{-4}	3.0×10^{-4}	–
			Filament 2			
CO_2	3.3×10^{-2}	5.2×10^{-2}	4.5×10^{-2}	3.0×10^{-3}	3.0×10^{-3}	4.2×10^{-3}
Ne	1.0×10^{-2}	1.1×10^{-2}	1.5×10^{-2}	7.9×10^{-4}	9.0×10^{-4}	1.4×10^{-3}
Xe	2.5×10^{-2}	2.2×10^{-2}	1.9×10^{-2}	1.1×10^{-3}	–	–

[a]Values are given in $mbar^{-1}$ for an electron emission current of 20 μA. The main mass peaks are m/q = 44 for CO_2, m/q = 20 for Ne, and m/q = 132 for Xe.

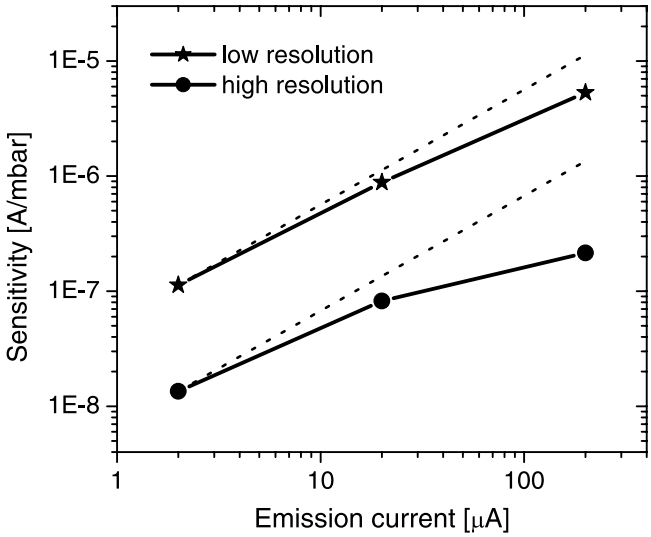

Figure 11. DFMS main mass peak sensitivity values for CO_2 (m/q = 44) as a function of the electron emission current. Results are presented for filament 1 in high- and low-mass resolution. All values have been measured with the Faraday cup. Dotted lines show the theoretically expected rise.

gauges and the electronic box. The instrument is shown in flight configuration except that the MLI is removed and the connector savers are still in place. The first gauge, labeled nude gauge, is mounted into a side wall of the electronic box pointing to the left. It is a hot filament extractor-type ionization gauge [*Redhead*, 1966]. Two 17 mm WRe (97:3) filaments (0.094 mm × 0.053 mm cross section) are available for redundancy, addressable by a switch as left and right filament. The emitted electrons are accelerated from the filament at a potential of +30 V toward a cylindrical inner anode grid set to +180 V. The gauge is decoupled from the surrounding plasma by an outer grid set to a potential of −12 V. Positively charged ions are still repelled by the inner grid. This gauge measures the total particle density with a nitrogen sensitivity of about 20 $mbar^{-1}$ at 100 μA electron emission current.

[41] The ram gauge is mounted perpendicular to the nude gauge on top of the housing, see also Figure 12. The incoming neutral gas is thermalized to a known temperature in the spherical equilibrium chamber. Afterward the particle density is again measured with an extractor-type ionization gauge. To allow a correct temperature measurement a microtip matrix is used as a cold electron source. The microtips, of the Spindt-type [*Meyer*, 1996; *Constancias*, 1998], were introduced into this type of setup by *Babtist et al.* [1996]. More than 1.8 million metallic microtips are mounted on a glass substrate arrayed by 32 × 32 pixels with an emitting area of about 13 mm × 13 mm. The matrix is divided into eight independent emitters which can be addressed separately.

[42] Each gauge has an electrometer to measure the current generated by the collected ions in the collector cathode. Both electrometers have three different ion current measurement modes. The low current range has the highest sensitivity and measures between 0.1 and 100 pA. For higher currents the electrometer is switched to the medium range, which is suitable for up to 10 nA. Above this limit the high range has to be used, although during the mission COPS will be switched off before the pressure reaches such high values. To increase the dynamic range of the gauges different emission modes are implemented. Both, the nude and the ram gauge can switch between high and low emission. In the low-emission mode the emission regulation can be set to electron emission currents between 2 and 20 μA, whereas in the high-emission mode, currents between 80 and 200 μA are possible.

4.4.2. Preliminary Calibration Results

[43] During the calibration of the COPS-FS sensor both gauges were mounted at CASYMIR. As the whole instrument does not fit inside the vacuum chamber of CASYMIR, both gauges had to be removed from the electronic box and assembled into a 6-way cross, see also Figure 13. Two additional flanges of the 6-way cross are used for a glass window and a Granville-Phillips Stabil-Ion (Series 370) ionization gauge. The electronic box is connected to a standard ROSINA-DPU (Digital Processing Unit) [*Balsiger et al.*, 2004] and the instrument is operated and controlled with an EGSE (Electrical Ground Support Equipment) computer with external 28 V supply and the GSEOS software [*Reiche et al.*, 2002].

[44] Due to very strict time constraints only static mode calibrations were performed. Pure argon in a pressure range from 5×10^{-10} to 10^{-6} mbar was used. The lower limit corresponds to the residual gas pressure. Each calibration point represents the mean value over 20 single measurements, taken within 40 s, of the ion current I_i and the electron emission current I_e. The pressure is propor-

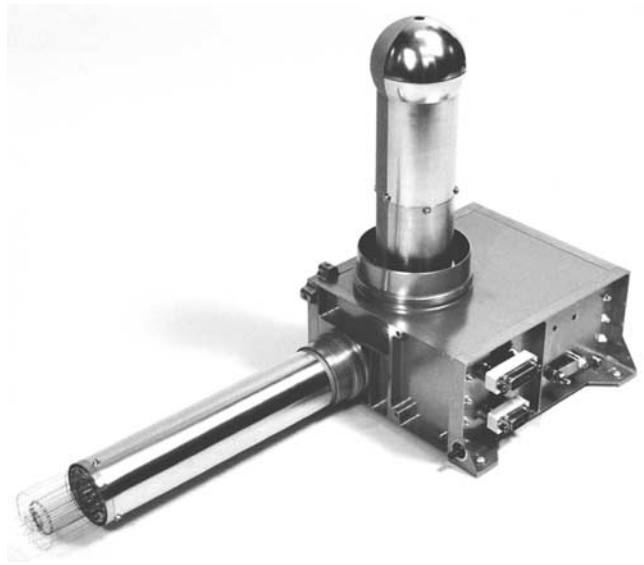

Figure 12. This image shows the ROSINA COPS-FS without the multilayer insulation. The ram gauge is mounted on top of the electronic box, and the nude gauge is pointing to the left. The electronic box has a length of about 17 cm.

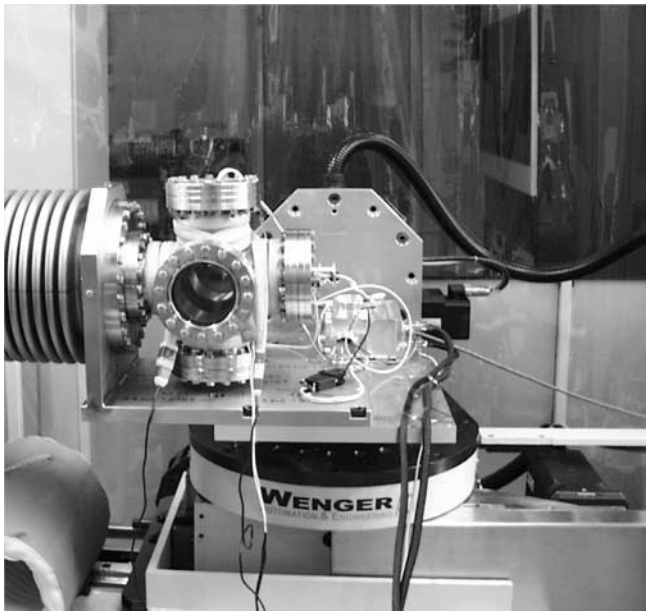

Figure 13. In this image the 6-way cross used for the COPS calibration is flanged at the docking adapter. The nude gauge is mounted at the top flange, and the ram gauge is mounted on the right side. Some parts of the five degrees of freedom positioning system of CASYMIR are visible below.

tional to the ratio between the ion current and the emission current:

$$\frac{I_\mathrm{i} - I_\mathrm{off}}{I_\mathrm{e}} = p(Ar) \times s, \tag{3}$$

where s is the instrument sensitivity. The electrometer offset values I_off have been measured before and after a single calibration set. Because of the residual gas in the vacuum chamber a calibration offset value r was added to equation (3) for the calibration fit:

$$\frac{I_\mathrm{i} - I_\mathrm{off}}{I_\mathrm{e}} = p(Ar) \times s + r. \tag{4}$$

To achieve a balanced error distribution over the whole pressure range the least squares fit was performed using relative errors:

$$\Delta^2 = \sum_k \left(\frac{p_k(Ar) \times s + r - \frac{I_{\mathrm{i},k} - I_{\mathrm{off},k}}{I_{\mathrm{e}k}}}{\frac{I_{\mathrm{i}k} - I_{\mathrm{off},k}}{I_{\mathrm{e}k}}} \right)^2. \tag{5}$$

The resulting sensitivity s will be used as the calibration factor for a specific gas. But if a high offset value r is obtained and the measurements are in a very low pressure region, the full linear equation should be used for exact measurements.

[45] The calibration results are presented in Figures 14 and 15 and in Table 2. Figure 14 shows the nude gauge results for the left filament in the high- and low-emission modes. The agreement with the Granville-Phillips Stabil-Ion reference gauge is very good over the full calibration range of almost four magnitudes, the rms error is only 1.3%. Between different calibration series the leak valve was fully closed to get readings for the residual gas pressures. Values between 5.3×10^{-10} to 8.6×10^{-10} mbar were obtained. In the high-pressure region above 10^{-7} mbar the low ion current range and the medium ion current range have been calibrated. The results from the least squares fits are summarized in Table 2. They show a small difference between the sensitivities of the different measurement modes. The rms error for a single fit is always less than 2%.

[46] So far, only the calibration factor is implemented in the ROSINA-DPU software. Therefore the accuracy of the low-pressure measurements is also somewhat limited by the calibration offset value r if no further data processing is performed. To have a reference for this lower limit, the offset value r can also be expressed as a pressure value $\frac{r}{s}$, yielding values between -3×10^{-12} to -2×10^{-9} mbar. The lower pressure limit with a maximum relative error ϵ can then be calculated as $p_\mathrm{low} = \frac{r}{|s\epsilon|}$. For example, with an allowed error of 15% pressure limits in the range of 2×10^{-11} to 1×10^{-8} mbar are obtained. These limits are so low that the proportional formula in the DPU software can be used without any significant loss of accuracy.

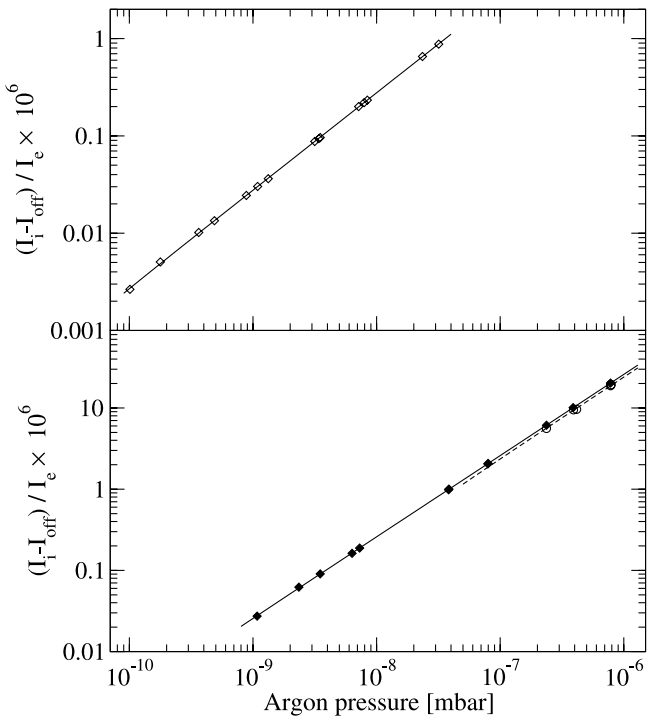

Figure 14. COPS-FS nude gauge calibration for the left filament. The high-emission-mode calibration at 100 μA electron emission current is given in the upper panel. The open diamonds represent the measured calibration points, and the least squares fit is plotted as the solid line. The lower panel shows the calibration results for the low-emission mode at 5 and 15 μA electron emission. Two ion current ranges have been used. The full diamonds show the calibration points for the low range, and the open circles represent the measurements with the medium ion current range. The residual gas pressure was between 5.9×10^{-10} to 1.9×10^{-9} mbar.

[47] The ram gauge calibration is given in Figure 15. The upper panel shows the measurements in the high-emission mode between 2×10^{-10} to 7×10^{-7} mbar argon pressure. Again a very good linearity was found with a rms error for the relative least squares fit of 0.005. The calibration points and the fit for the low-emission mode are plotted in the lower panel of Figure 15. This fit has a rms error of 0.036, which is the largest error of all calibration calculations. The plot in Figure 15 shows some differences between the fit curve and the calibration points in the low-pressure region below 10^{-8} mbar. Due to the smaller anode grid the ram gauge sensitivity is roughly four times lower as compared to the nude gauge, see also Table 2. Therefore low-pressure measurements with the ram gauge are more sensitive to internal or external interferences. The calculated low-pressure limits based on an error of 15% are 2×10^{-10} and 6×10^{-10} mbar for the high- and low-emission modes. Although these values are higher than the corresponding nude gauge limits the use of a calibration factor only is still sufficient, as the low-emission mode will not be used in the low-pressure region.

5. Summary and Conclusions

[48] CASYMIR was designed and built as a calibration facility for the ROSINA instrument package. The main goal is the simulation of the neutral gas atmosphere around a cometary nucleus. The system can provide static environments in a pressure range from 5×10^{-10} to 10^{-5} mbar and molecular beam intensities between 10^{12} to 10^{15} $cm^{-2}s^{-1}$ with expansion velocities of 300 to 3000 m s^{-1}. Although CASYMIR was built for ROSINA its design is flexible enough to be used as a calibration facility for other instruments or it could be adapted to other experimental setups.

[49] During the first ROSINA calibration period all three sensors were calibrated in the static mode with different species, e.g., CO_2 and several noble gases. This campaign has shown that a dedicated calibration system is a necessity to fulfill the strict calibration time constraints during the building and delivery phase of scientific instruments for space mission.

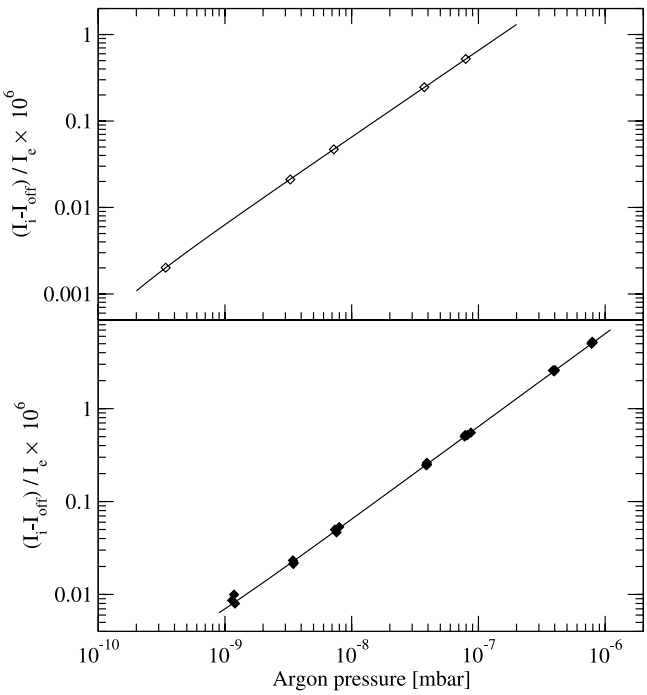

Figure 15. COPS-FS ram gauge calibration with argon. The upper panel shows the calibration for the high-emission mode at 100 μA with all eight microtip groups running. Open diamonds mark the calibration points, and the fit is given by the solid line. The results for the low-emission mode at 5 and 15 μA electron emission current are presented in the lower panel. The calibration measurements are plotted with diamonds, and the solid line shows the least squares fit. During this calibration a residual gas pressure between 4.8×10^{-10} and 5.1×10^{-10} mbar was measured.

Table 2. Argon Calibration of the COPS-FS Nude Gauge and Ram Gauge[a]

Emission Mode	Ion Range	Sensitivity s	Calibration Offset r	rms Error
		Nude Gauge		
High, 100 μA	low	27.75	-8.72×10^{-11}	0.013
Low, 5 and 15 μA	low	25.92	-3.39×10^{-10}	0.0088
Low, 5 and 15 μA	medium	24.02	-4.87×10^{-8}	0.019
		Ram Gauge		
High, 100 μA	low	6.55	-2.24×10^{-10}	0.0045
Low, 5 and 15 μA	low	6.40	-5.98×10^{-10}	0.036

[a]The sensitivity factors s (in $mbar^{-1}$) and the calibration offset values were obtained by a least squares fit of the relative errors.

[50] **Acknowledgments.** This work was supported by the ESA PRODEX programme and the Swiss National Science Foundation. We gratefully acknowledge the whole ROSINA-Team [cf. *Balsiger et al.*, 2004] for building the ROSINA instrument. We are also indebted to all coworkers from the engineering office, the mechanical and electrical workshops who have been involved in the successful completion of this project.

References

Altwegg, K., H. Balsiger, and J. Geiss (1999), Composition of the volatile material in Halley's coma from in situ measurements, *Space Sci. Rev.*, *90*, 3–18.

Ashkenas, H., and F. S. Sherman (1966), The structure and utilization of supersonic free jets in low density wind tunnels, in *Advances in Applied Mechanics*, vol. II, suppl. 3, *Rarefied Gas Dynamics*, edited by J. H. de Leeuw, Academic, San Diego, Calif.

Babtist, R., C. Bieth, and C. Py (1996), A bayard-alpert vacuum gauge with microtips, *J. Vac. Sci. Technol. B*, *14*, 2119–2125.

Balsiger, H., et al. (1997), Rosetta Orbiter Spectrometer for Ion and Neutral Analysis: ROSINA, *Adv. Space Res.*, *21*, 1527–1535.

Balsiger, H., et al. (2004), ROSINA: Rosetta Orbiter Sspectrometer for Ion and Neutral Analysis, *Eur. Space Agency Spec. Publ.*, *ESA-SP 1165*, in press.

Berner, C., L. Bourillet, J. Casteren, J. Ellwood, M. Kasper, P. Kletzine, R. Schulz, G. Schwehm, M. Warhaut, and P. Bond (2002), Rosetta: ESA's comet chaser, *ESA Bull.*, *112*, 10–37.

Colom, P., E. Gérard, C. Crovisier, and D. Bockelée-Morvan (1998), Observations of the oh-radicals in comet C/1995 O1 (Hale-Bopp) with the Nancy radio telescope, paper presented at Proceedings of the First International Conference on Comet Hale-Bopp, Comet Hale-Bopp Eur. Team, Puerto de la Cruz, Tenerife, Spain.

Combi, M. R., A. L. Cochran, W. D. Cochran, D. L. Lambert, and C. M. Johns-Krull (1999), Observation and analysis of high-resolution optical line profiles in comet Hyakutake (C/1996 B2), *Astrophys. J.*, *512*, 961–968.

Constancias, C. (1998), Electron field emission with microtips for flat panel displays: Simulations, characterisations and experimental comparisons, Ph.D. thesis, Université de Grenoble, Saint Martin d'Heres, France.

Crovisier, J. (1998), Infrared observations of volatile molecules in comet Hale-Bopp, paper presented at Proceedings of the First International

Conference on Comet Hale-Bopp, Comet Hale-Bopp Eur. Team, Puerto de la Cruz, Tenerife, Spain.
Crovisier, J., and D. Bockelée-Morvan (1999), Remote observations of the composition of cometary volatiles, *Space Sci. Rev.*, *90*, 19–32.
Crovisier, J., K. Leech, D. Bockelée-Morvan, T. Y. Brooke, M. S. Hanner, B. Altieri, H. U. Keller, and E. Lellouch (1997), The spectrum of comet Hale-Bopp (C/1995 O1) observed with the Infrared Space Observatory at 2.9 AU from the Sun, *Science*, *275*, 1904–1907.
Ghielmetti, A., H. Balsiger, R. Bänninger, P. Eberhardt, J. Geiss, and D. Young (1983), Calibration system for satellite and rocket-borne ion mass spectrometers in the energy range from 5 ev/charge to 100 kev/charge, *Rev. Sci. Instrum.*, *54*, 425–436.
Hohl, M., P. Wurz, S. Scherer, K. Altwegg, and H. Balsiger (1999), Mass selective blanking in a compact multiple reflection time-of-flight mass spectrometer, *Int. J. Mass Spectrom.*, *188*, 189–197.
Johnson, E. G., and A. O. Nier (1953), Angular aberrations in sector shaped electromagnetic lenses for focusing beams of charged particles, *Phys. Rev.*, *91*, 10–17.
Lämmerzahl, P., et al. (1987), Expansion velocity and temperatures of gas and ions measured in the coma of comet P/Halley, *Astron. Astrophys.*, *187*, 169–173.
Loose, A. (2002), Description of the equivalent time sampling system (ETS and ETSL) of the Rosina RTOPF instrument (revision 1.4), Max-Planck-Inst. für Aeron., Katlenburg-Lindau, Germany.
Mattauch, J., and R. Herzog (1934), Über einen neuen massenspektrographen, *Z. Phys.*, *89*, 786–795.
Matuschek, O., W. Böker, H. Sommer, and A. Lagg (2001a), Gas calibration unit (GCU) RTOF FS endtest, Max-Planck-Inst. für Aeron., Katlenburg-Lindau, Germany.
Matuschek, O., H. Sommer, and A. Lagg (2001b), Gas calibration unit (GCU) DFMS FS endtest, Max-Planck-Inst. für Aeron., Katlenburg-Lindau, Germany.
Meyer, R. (1996), Procédé de fabrication de micropointes métalliques, *Vide*, *282*, 478–484.
Redhead, P. A. (1966), New hot-filament ionization gauge with low residual current, *J. Vac. Sci. Technol.*, *3*, 173–180.
Reiche, K.-U., H. Schmidt, K. Stöcker, and T. Wittrock (2002), Ground support equipment operating system, IDA, Tech. Univ. of Braunschweig, Braunschweig, Germany.
Scherer, S. (1999), Design of a high-performance reflectron time-of-flight mass spectrometer for space applications, Ph.D. thesis, Univ. of Bern, Bern.
Schletti, R., P. Wurz, S. Scherer, and O. Siegmund (2001), Fast microchannel plate detector with an impedance matched anode in suspended substrate technology, *Rev. Sci. Instrum.*, *72*, 1634–1639.
Scoles, G. (1988), *Atomic and Molecular Beam Methods*, vol. 1, Oxford Univ. Press, New York.
Weaver, H. A., P. D. Feldman, M. F. A'Hearn, C. Arpigny, J. C. Brandt, M. C. Festou, M. Haken, J. B. McPhate, S. A. Stern, and G. P. Tozzi (1997), The activity and size of the nucleus of comet Hale-Bopp (C/1995 O1), *Science*, *275*, 1900–1904.
Weaver, H. A., P. D. Feldman, M. F. A'Hearn, C. Arpigny, J. C. Brandt, and S. A. Stern (1998), Hubble Space Telescope observations of comet Hale-Bopp, paper presented at Proceedings of the First International Conference on Comet Hale-Bopp, Comet Hale-Bopp Eur. Team, Puerto de la Cruz, Tenerife, Spain.
Westermann, C. (2000), A novel calibration system for the simulation of cometary atmospheres, Ph.D. thesis, University of Bern, Bern.
Westermann, C., W. Luithardt, E. Kopp, T. Koch, R. Liniger, H. Hofstetter, J. Fischer, K. Altwegg, and H. Balsiger (2001), A high precision calibration system for the simulation of cometary gas environments, *Meas. Sci. Technol.*, *12*, 1594–1603.

K. Altwegg, H. Balsiger, S. Graf, A. Jäckel, E. Kopp, U. Langer, W. Luithardt, C. Westermann, and P. Wurz, Physikalisches Institut, Universität Bern, Sidlerstrasse 5, CH-3012 Bern, Switzerland. (stephan.graf@phim.unibe.ch)